Solar Energy Vol. 42, No. 6, pp. 441–447, 1989
Printed in the U.S.A.

0038–092X/89 $3.00 + .00

THE EFFECT OF PHASE-CHANGE MATERIAL PROPERTIES ON THE PERFORMANCE OF SOLAR AIR-BASED HEATING SYSTEMS

A. A. GHONEIM
Laboratory of Physics, Mathematical Eng. and Eng. Physics Dept.
Faculty of Engineering, University of Alexandria
Alexandria, Egypt

and

S. A. KLEIN
Solar Energy Laboratory, University of Wisconsin-Madison
Madison, WI 53706, U.S.A.

1. INTRODUCTION

Considerable attention has been devoted to the development of phase-change energy storage (PCES) units for solar heating and cooling systems. This work has been motivated by the significant reduction in storage volume which can be achieved with PCES compared to sensible heat storage using air as the heat transfer fluid. The melting temperature and latent heat of the phase-change material (PCM) characterize the PCES substance. The effect of phase-change material melting temperature and latent heat has been studied by Jurinak *et al.* [1,2]. Their main conclusion was that the PCM should be selected on the basis of its melting temperature, rather than its latent heat, i.e., the melting temperature has a significant effect on system performance. Their results are based on a heating season simulation from October 1–May 1 in Madison (Wisconsin).

There are many factors which affect system performance such as, the average temperature of the storage unit, the fraction of time that the storage unit is charged, the fraction of time that the storage unit is discharged, the fraction of time that the storage unit is isolated, and the fraction of total time that the storage unit operates in the two-phase mode. These factors depend primarily on the amount of incident solar energy relative to the heating load. To determine the effect of thermal properties on system performance, a simuation study must be conducted for different ratios of incident solar energy to heating load and a variety of climate types.

PCM's may be inorganic salts or paraffin wax. A major drawback to paraffins for PCES is their flamability and the relatively high expense of the processes needed to produce chemically pure paraffins from the petroleum (industrial) grade paraffins. Chemically pure paraffins have a high latent heat, on the order of 200 kJ/kg, and they melt at a uniform melting temperature. On the other hand, the latent heat of the petroleum grade paraffins is roughly 75% that of the pure compound[3], and they melt semi-congruently (i.e., the PCM melts over a temperature bandwidth around the nominal melting temperature). The extent to which the petroleum grade paraffins can be used without significantly decreasing the fraction of the heating load met by solar energy has not been previously studied.

The main objectives of the present study are to

1. Investigate the effect of melting temperature and latent heat for different storage masses on solar-system performance for different ratios of incident solar energy to heating load
2. Study the previous effect for several climates (different locations)
3. Compare the performance of solar heating systems utilizing industrial grade and pure paraffins.

The effect of PCES on the performance of water-based systems was examined in [4,5]. It was found that, compared to sensible heat storage with water, there were no significant performance gains (or storage size reduction) resulting from using PCES with water-based systems. The effect of using different models on the performance of solar heating systems was examined in [5]. It was found that, with air-based systems, little error in the calculated system performance results from the use of the simplified infinite NTU model of Morrison *et al.*[4] after taking heat storage losses into consideration. The present study will be limited to air-based systems utilizing PCES and will be based on results from infinite NTU model.

2. SYSTEM CONFIGURATION AND CONTROL STRATEGY

The transient simulation program TRNSYS[6] is used to determine the performance of the standard solar air space system shown in Fig. 1. The parameters selected for the system components are listed in Table 1. The system shown in Fig. 1 has three modes of operation. The first mode occurs when solar energy is available for collection and there is a space heating load. During this mode, the fluid is circulated

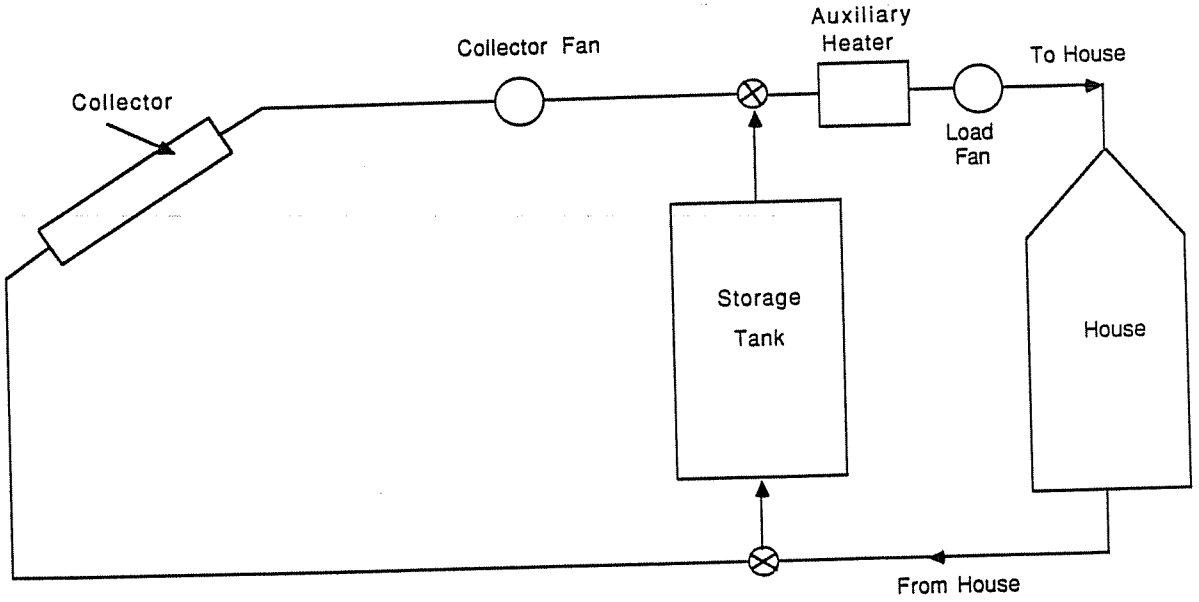

Fig. 1. Schematic representation of the standard solar air heating system.

between the collectors and the load while the storage unit is isolated. The second mode occurs when solar energy is available for collection and there is no space heating load. In this case, air is circulated between the collectors and the storage units. The final mode occurs when solar energy is not available for collection and there is a space heating load. In this case, air is circulated between the storage unit and the load. The system operation is controlled by a series of thermostats, fans, and flow diverters. Air flow to the space heating load and auxiliary heat is governed by a two-stage thermostat which monitors room temperature. It commands first-stage (solar source) heating when the room temperature drops below 20°C, and second-stage (auxiliary source) heating when the room temperature drops below 18.5°C.

Table 1. Air-based system parameters[7,8]

Collector	
Number of glass covers	2
Product of extinction coefficient and thickness of each glass cover	0.037
Refractive index	1.526
Collector plate absorptance (α)	0.95
Collector emittance (ϵ)	0.9
$F_R(\tau\alpha)_n$	0.6
$F_R U_L$	12 kJ/hm^{2}K
Mass flow rate per unit collector area	44 kg/hm^2
Glazing spacing	0.04 m
Ducts	
The collector circuit pipings and the heating circuit piping are divided into a cold and a hot side, and the following data are the same for both sides	
Collector circuit pipe (each side)	
Length	20 m
Diameter	0.04 m
Heat loss	20 kJ/hK
Fluid density	1.204 kg/m3
Fluid specific heat	1.012 kJ/kgK
Ambient temperature	20°C
Heating circuit pipe (each side)	
Length	15 m
Diameter	0.04 m
Heat loss	15 kJ/hK
Fluid density	1.204 kg/m^3
Fluid specific heat	1.012 kJ/kgK
Ambient temperature	20°C

3. RESULTS AND DISCUSSION

Simulations of air-based PCES systems were conducted for five locations, namely Madison (Wisconsin), Great Falls (Montana), Columbia (Missouri), Charleston (South Carolina), Albuquerque (New Mexico), and for two different heating season months (January and March). The mass flow rate per unit collector area, collector area, heat removal factor-collector overall loss coefficient product, and system control strategy are assumed to be the same for all the simulations carried out in this study. Simulation results are presented as a function of Y, where

$$Y = A_c F_R(\overline{\tau\alpha})\overline{H}_T N/L_S \tag{1}$$

A_c is the area of the solar collector (m^2); F_R is the collector heat removal factor; $(\overline{\tau\alpha})$ is the collector monthly average transmittance-absorptance product; $\overline{H}_T$ is the monthly average daily radiation incident on the collector surface per unit collector area (kJ/m^2); N is the number of days in the month; L_S is the monthly space heating load (kJ). The equation for Y can be rewritten in a more convenient form for calculations[9]:

$$Y = F_R(\tau\alpha)_n \cdot \frac{(\overline{\tau\alpha})}{(\tau\alpha)_n} \cdot \overline{H}_T A_c N/L_S \tag{2}$$

where, $(\tau\alpha)_n$ is the collector monthly average transmittance-absorptance product at normal incidence. The monthly average daily radiation incident on the collector surface per unit collector area ($\overline{H}_T$) could be calculated from montly global horizontal data as described in[7], but in this study, $\overline{H}_T$ was calculated by hourly TRNSYS simulations and used to evaluate Y. The value of $F_R(\tau\alpha)_n$ can be calculated from standard ASHRAE collector tests[10]. The ratio $(\overline{\tau\alpha})/(\tau\alpha)_n$ was assumed to be 0.94 for a two-cover collector for the heating season months when the collector is tilted within 15°C of the latitude[9]. The space heating load, for a small thermal capacitance building, is approximately equal to (UA*DD). The loss coefficient-area product (UA) of the building was varied in this study. The number of degree-days in the month, DD, in °C-days, is calculated on a 18.3°C base.

The density, specific heat, and thermal conductivity of the PCM are assumed to be equal to the corresponding values for paraffin wax. A wax was chosen because a member of the paraffin family can be found which melts at any desired temperature. In addition, paraffins do not supercool, do not degrade with repeated cycling, and are generally stable which offsets their disadvantage of having a much lower density than salt hydrates. For space heating applications, the melting temperature is bounded by the room temperature (20°C) and approximately 50°C. In the present study, melting temperature is varied from 30°C to 50°C. The minimum utilization temperature of the solar system, assumed here to be 30°C, represents a constraint on the temperature of the airstream supplied to meet the space heating load in order to assure comfort. The minimum solar source airstream temperature must be larger than the minimum utilization temperature to an extent dependent on heat exchanger size. The variation of the PCM melting temperature at constant latent heat can be closely approximated by substituting various paraffins. The latent heat of candidate phase-change material was varied between 129–289 kJ/kg[11]. A schematic representation of the PCES unit is shown in Fig. 2. The storage unit composed of a number of rectangular cross-sectioned channels for the flowing fluid, connected in parallel and separated by the phase-change material (PCM).

Figure 3 shows the variation of the solar fraction with melting temperature at different storage masses (10, 20, and 40 kg/m^2) and for different values of Y(0.7, 1.0, and 2.0). The lines shown in this and following figures are the average results from the five locations. The maximum standard deviation between the calculated performance and the plotted lines in Figs. 3–7 is about 0.7%. For values of Y up to 0.6, the melting temperature and latent heat have no effect on the solar fraction. At these low values of Y, the average temperature of the storage unit does not exceed 25°C for the melting temperature range (30–50°C) and latent heat range (129–289 kJ/kg) used in this study, i.e., the PCES unit is acting as a sensible store. For values of Y greater than 0.6, the solar fraction decreases with increasing melting temperature because the average temperature of the storage unit increases, increasing the average collector inlet temperature, which decreases the collector efficiency. As seen from Fig. 3, the optimum melting temperature is equal to the minimum utilization temperature independent of the storage mass.

Changing the melting temperature from 30–50°C at the nominal latent heat (209 kJ/kg) for the different storage masses used results in decreasing the solar fraction. This decrease is more pronounced for the values of Y between 0.6 and 1.0. For example, changing the melting temperature from 30–50°C at the nominal latent heat, and using a storage mass of 20 kg/m^2 results in a reduction in solar fraction of

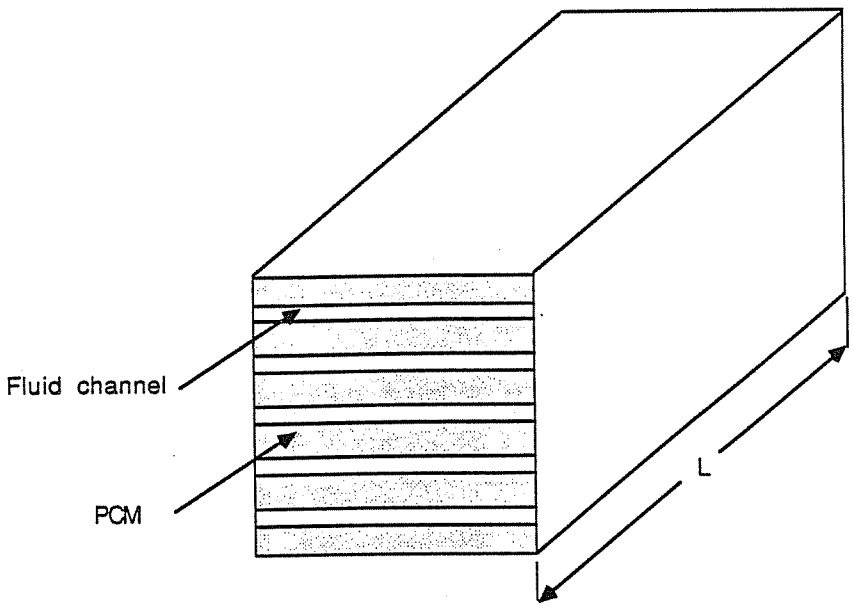

Fig. 2. Schematic representation of (PCES) unit.

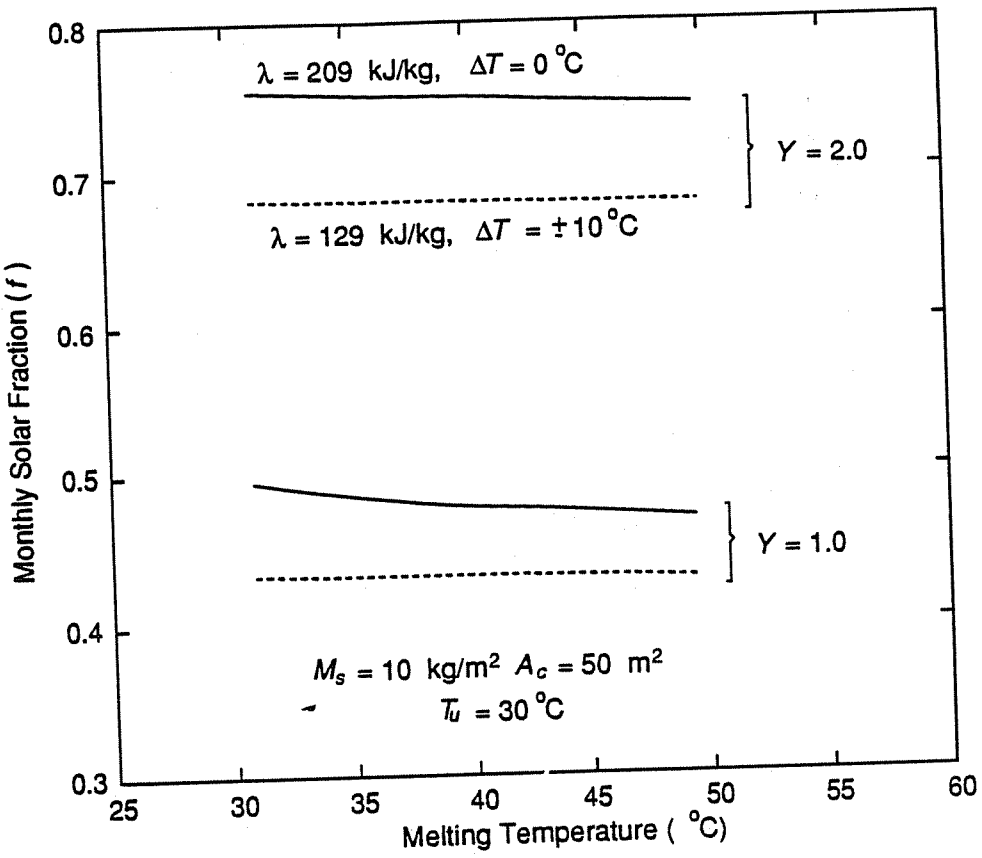

Fig. 3. Variation of monthly solar fraction with melting temperature and storage mass.

approximately 2.0, and 2.9% of the load for values of Y equal to 0.7 and 1.0 respectively. These changes represent approximately 5.0% of solar fraction range for each case. As the value of Y increases above 1.0, the effect of melting temperature is reduced. At values of Y equal to or greater than 2.0, the effect of melting temperature becomes negligible. For example, changing the melting temperature from 30–50°C at the nominal latent heat decreases the solar fraction by 1% of the load for storage mass equal to 20 kg/m^2 (1.2% of the scale). At high values of Y, the PCM is almost always in a liquid state and again acts like a sensible store. These results indicate that the melting temperature has a significant effect on the thermal performance of the solar system for values of Y only between 0.6 and about 1.0.

Figure 4 shows the variation of solar fraction with latent heat at different storage masses for different values of Y (0.7, 1.0, and 2.0). As the latent heat increases, the amount of energy stored in the material increases and this subsequently increases the solar fraction. At the smallest storage mass used (10 kg/m^2), the latent heat has a significant effect on the performance of the solar system for all values of Y. For example, at storage mass equal to 10 kg/m^2, and melting temperature equal to the minimum utilization temperature ($T_m = T_u = 30$°C), increasing the latent heat from its lowest value (129 kJ/kg) to its highest value (289 kJ/kg), increases the solar fraction by 3.2, 4.5, and 7.2% of the load for values of Y equal to 0.7, 1.0, and 2.0, respectively. The latent heat has a larger effect on the performance of the solar systems with smaller storage masses. As the storage mass increases, this change becomes less important for values of Y up to 1.0. For values of Y equal to or greater than 2.0, the latent heat becomes significantly important for all storage masses.

To confirm the previous results, the effect of the average temperature of the storage unit, and the fraction of time that the storage unit operates in the two-phase mode were studied. At values of Y up to 1.0, the average temperature of the storage unit is on the order of the melting temperature. For values of Y equal to or greater than 2.0, the average temperature of the storage unit is significantly higher than the average temperature of the range used for melting temperature. For example, at melting temperature equal to 30°C, latent heat equal to the nominal value (209 kJ/kg), and storage mass equal to 20 kg/m^2, the average temperatures of the storage unit are found to be 30, 49, and 57°C for values of Y equal to 1.0, 2.0, and 2.5, respectively. At the same conditions, the fraction of time that the storage unit operates in the two-phase mode are 0.45, 0.72, and 0.79, respectively. For values of Y equal to or greater than 2.0, the temperature of the storage unit is significantly higher than the storage temperature of the range used for melting temperatures, and the storage unit operates most of the time in the two-phase mode. For these values of Y, the melting temperature has no significant effect on the solar fraction.

To compare between the industrial grade and pure

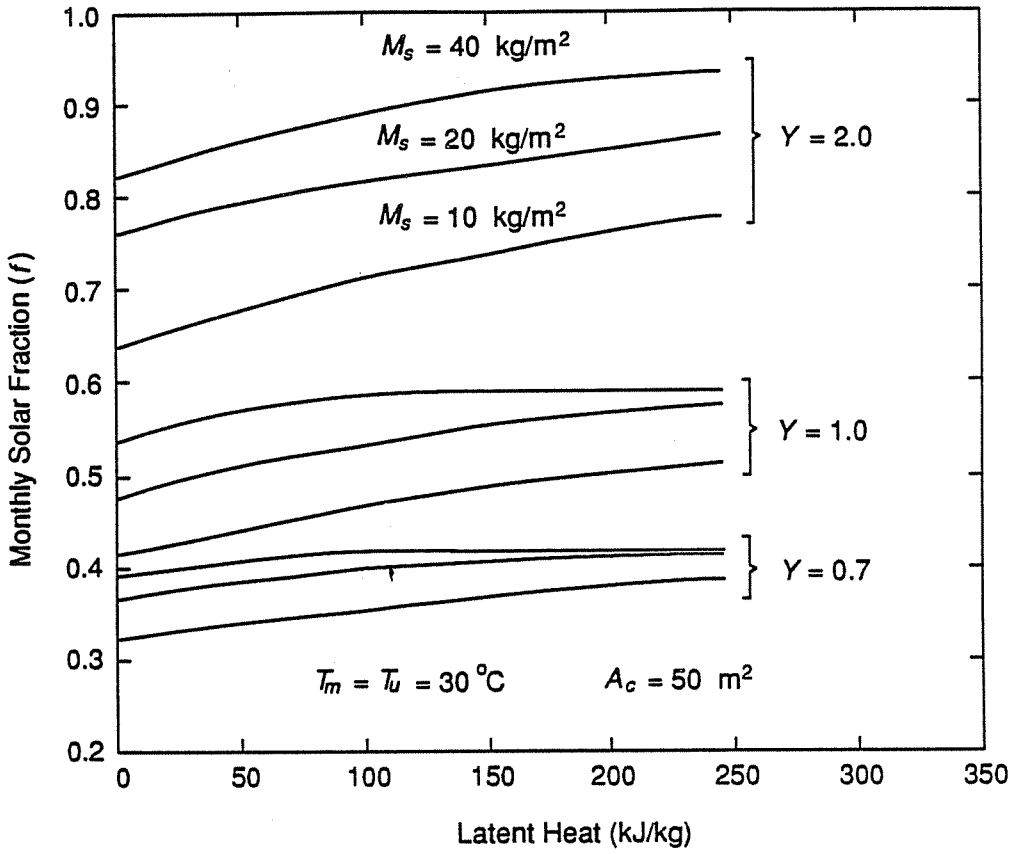

Fig. 4. Variation of monthly solar fraction with latent heat and storage mass.

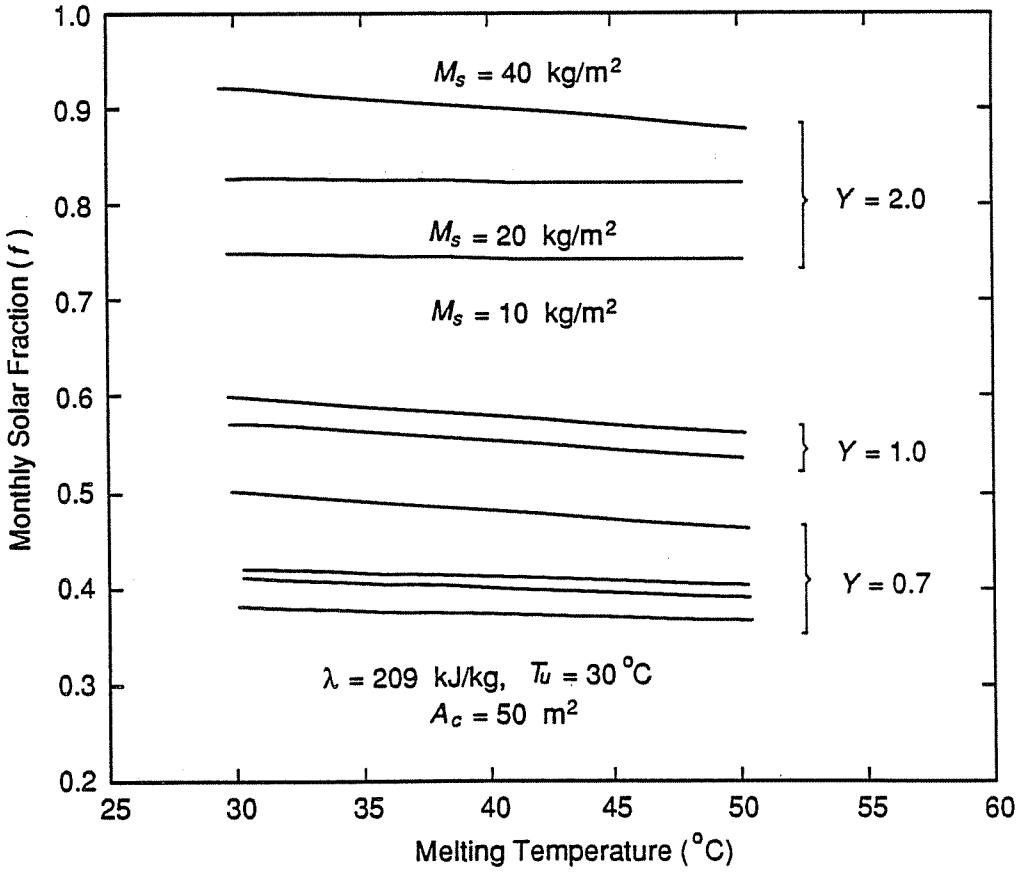

Fig. 5. Comparison of the monthly solar fraction of solar heating systems utilizing industrial grade and pure paraffins.

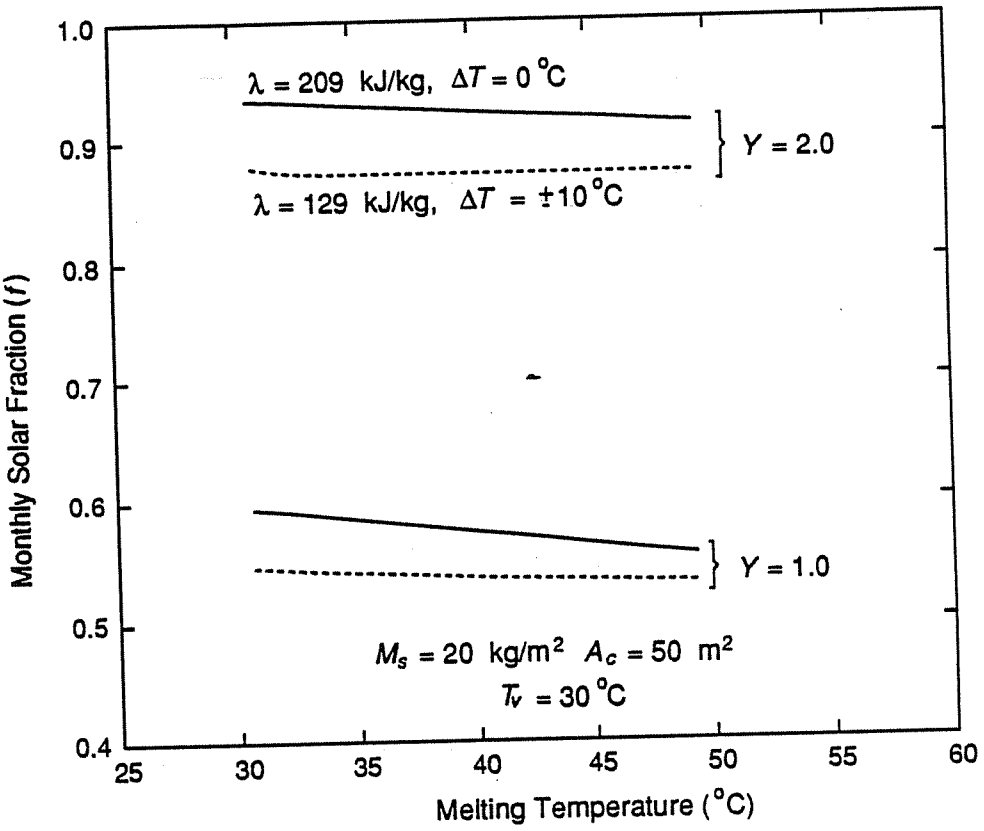

Fig. 6. Comparison of the monthly solar fraction of solar heating systems utilizing industrial grade and pure paraffins.

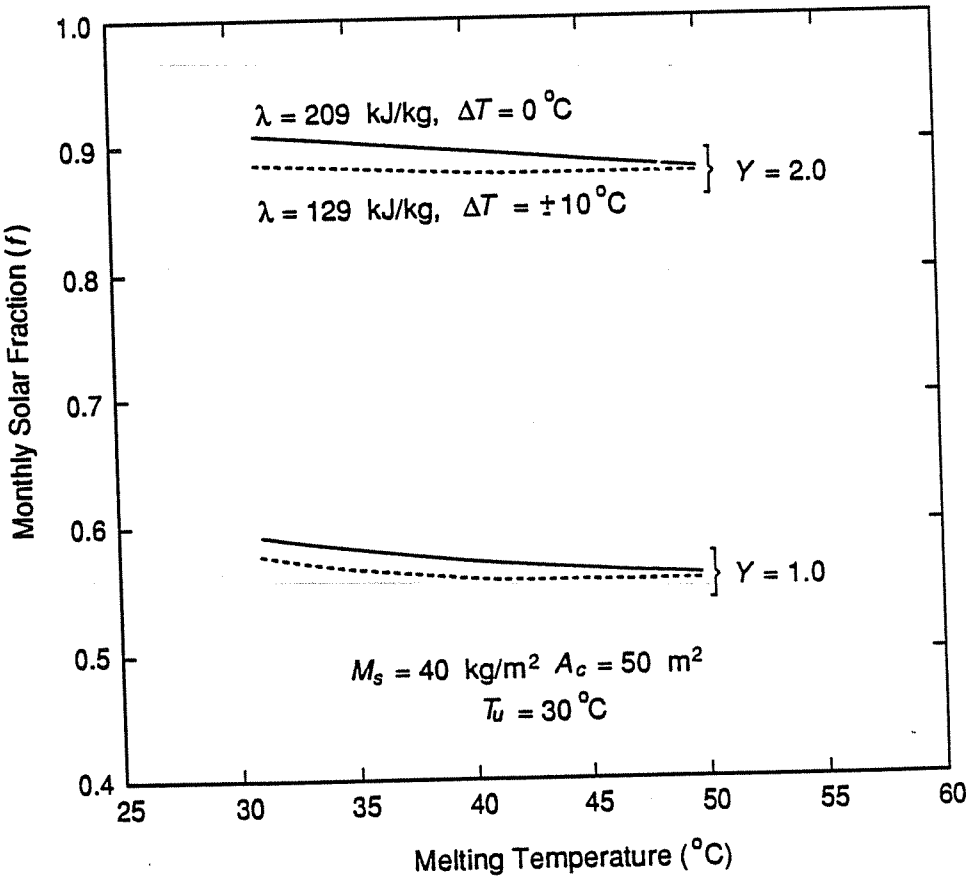

Fig. 7. Comparison of the monthly solar fraction of solar heating system utilizing industrial grade and pure paraffins.

paraffins, the industrial grade paraffins were assumed to have a melting temperature bandwidth of 20°C ($\Delta T = T_{m1} - T_{m2} = 20$°C, where T_{m1}, and T_{m2} are the lower and upper limits of PCM melting temperature, respectively), i.e., ± 10°C around the nominal melting temperature. Figures 5–7 show the variation of the solar fraction for industrial grade (λ = 129 kJ/kg, ΔT = ± 10°C) and pure paraffins (λ = 209 kJ/kg, ΔT = 0°C), for two values of Y (1.0, and 2.0) at different storage masses (10, 20, and 40 kg/m^2). At storage mass equal to 10 kg/m^2, the use of industrial grade paraffins results in significantly lower solar fraction as seen in Fig. 5. The difference between industrial grade and pure paraffins becomes smaller as storage mass is increased. At storage mass equal to 40 kg/m^2, similar thermal performance is obtained with either type of paraffin.

In conclusion, the results indicate that, for solar system design with small values of the ratio of incident solar energy to the heating load (values of Y less than about 1.0) and storage mass greater than 10 kg/m^2, the melting temperature has a greater effect on the thermal performance of the solar system than the latent heat. For these solar system designs, the candidate PCM should be chosen in the basis of its melting temperature only. On the other hand, for solar systems with a high value of the ratio of incident solar energy to the heating load (values of Y equal to or greater than about 2.0), the latent heat of the PCM has a greater effect on the thermal performance of the solar system than does the melting temperature, contrary to the conclusion reached by Jurinak *et al.*[1,2]. Also the petroleum grade paraffins (with λ = 129 kJ/kg, and melting temperature bandwidth of up to ± 10°C around the nominal melting temperature), for storage masses equal to or greater than 20 kg/m^2 can be used directly for PCES with little decrease in the solar fraction, taking advantage of their reduced cost. There is no need to seek candidate PCM for such conditions. Calculations have been done for the five locations and the results, presented in terms of Y, appear to be location independent.

Acknowledgments—The authors would like to express appreciation to Professor J. A. Duffie, Director of the Solar Energy Laboratory at the University of Wisconsin-Madison, for allowing the use of Solar Laboratory facilities. The financial support of the Egyptian government during this study is acknowledged.

NOMENCLATURE

- A_c collector area
- c_f specific heat of the circulating fluid
- DD the number of degree-days in the month
- F monthly solar fraction.
- F_R collector heat removal factor
- h total heat transfer loss coefficient
- H_T monthly average daily solar radiation incident on the collector surface
- L length of (PCES) unit in the flow direction
- L_S monthly space heating load
- $\dot{m}$ mass flow rate
- M_s PCM mass per unit collector area
- N number of days in the month
- NTU number of transfer unit ($NTU = hPL/\dot{m}c_f$)
- P Perimeter of the storage material
- T_m PCM finite melting temperature
- T_{m1} lower limit of PCM melting temperature
- T_{m2} upper limit of PCM melting temperature
- T_u minimum utilizing temperature
- ΔT PCM melting temperatre bandwidth
- UA loss coefficient-area product
- λ latent heat of PCM
- ρ PCM density
- $(\overline{\tau\alpha})$ collector monthly average transmittance-absorptance product
- $(\tau\alpha)_n$ collector monthly average transmittance-absorptance product at normal incidence

REFERENCES

1. J. J. Jurinak and S. I. Abdel Khalik, Properties optimization for phase-change energy storage in air-based solar heating system. *Solar Energy* **21,** 377–383 (1978).
2. J. J. Jurinak and S. I. Abdel Khalik, On the performance of air-based solar heating systems utilizing phase-change energy storage. *Solar Energy* **24,** 503–522 (1979).
3. B. Shelpuk, P. Joy, and M. Crouthamel, Technical and economic feasibility of thermal storage final report, C00/2591-76/1, RCA Advanced Technology Laboratories, Candem, N.J. (1976).
4. D. J. Morrison and S. I. Abdel Khalik, Effect of phase-change energy storage on the performance of air-based and liquid-based solar heating systems. *Solar Energy* **20,** 57–67 (1978).
5. A. A. Ghoneim, Comparison of theoretical models of phase-change and sensible heat storage for air and water-based solar heating systems. (in press).
6. S. A. Klein *et al.* TRNSYS, A transient simulation program, University of Wisconsin-Madison, version 12.2 (1988).
7. J. A. Duffie, and W. A. Beckman, *Solar energy thermal processes*. Wiley Interscience, New York (1980).
8. H. P. Garg *Advances in solar energy technology,* vol. 2, D. Reidel Publishing Company, Holland (1987).
9. W. Beckman, S. Klein, and J. Duffie, *Solar heating design by the F-chart method.* Wiley Interscience, New York (1977).
10. ASHRAE, Standard 93-77, American Society of Heating, Refrigeration, and Air Conditioning Engineers, New York (1977). "Methods of Testing to Determine the Thermal Performance of Solar Collectors."
11. D. Hale, M. Hoover, and M. O'Neill, Phase Change-Materials Handbook, NASA CR-61363, NASA George C. Marshall Space Flight Center (1971).